

See discussions, stats, and author profiles for this publication at: <https://www.researchgate.net/publication/265128656>

New two- and three-cationic polymethine dyes. Synthesis, properties and application

ARTICLE *in* DYES AND PIGMENTS · JANUARY 2015

Impact Factor: 3.97 · DOI: 10.1016/j.dyepig.2014.06.016

CITATION

1

READS

47

2 AUTHORS, INCLUDING:

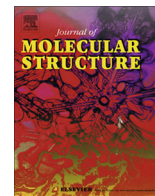


Janina Kabatc

University of Technology and Life Sciences ...

71 PUBLICATIONS 647 CITATIONS

SEE PROFILE



New *N*-(carboxyethyl)-2-methylbenzothiazole-based hemicyanine dyes: Synthesis, spectra, photostability and association with bovine serum albumin



Janina Kabatc^{a,*}, Katarzyna Jurek^a, Łukasz Orzeł^b

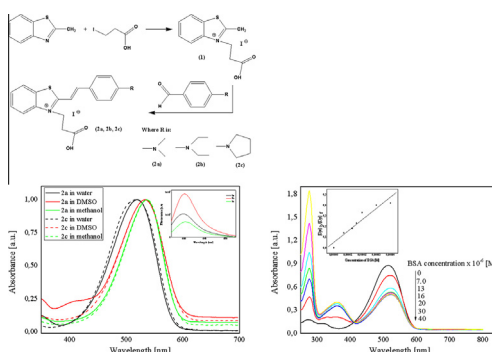
^a University of Technology and Life Sciences, Faculty of Chemical Technology and Engineering, Seminaryjna 3, 85-326 Bydgoszcz, Poland

^b Jagiellonian University, Faculty of Chemistry, Ingardena 3, 30-060 Cracov, Poland

HIGHLIGHTS

- The synthesis of new *N*-(carboxyethyl)-2-methylbenzothiazole derivatives.
- Spectroscopic, electrochemical properties, photostability, aggregation, association.
- New dyes as spectroscopic probes for biomolecules determination.

GRAPHICAL ABSTRACT



ARTICLE INFO

Article history:

Received 13 November 2014

Received in revised form 9 December 2014

Accepted 9 December 2014

Available online 18 December 2014

Keywords:

Hemicyanine dyes

Aggregation

Photostability

Association

ABSTRACT

Three hemicyanine dyes containing *N*-(carboxyethyl)-2-methylbenzothiazolium group and bearing different substituent in *p*-position of phenyl ring of styryl moiety were readily prepared by a Knoevenagel condensation. Their UV/Vis and fluorescence spectra, aggregation, photostability and association with bovine serum albumin were studied. The maximum absorption and emission wavelengths of the dyes in different solvents were in the range 520–620 nm. Compared with a typical *N*-alkyl-2-methylbenzothiazolium hemicyanine dyes, the introduction of carboxyethyl group reduced aggregation and improved molar extinction coefficient, and photostability in water. These dyes may envisioning their potential usefulness for photodynamic therapy. The spectroscopic characterization of all the dyes synthesized is also described.

© 2014 Elsevier B.V. All rights reserved.

Introduction

Cyanine dyes have been extensively studied over the past century, mainly as photosensitizers for photography [1–4]. In recent decades, other applications such as visible and near-infrared laser dyes [5–7], optical recording and storage media [4,5], biological fluorescent stains and probes [8], among others, have added

renewed interest to the study and development of this family of dyes.

Since the end of the 1980s, cationic dyes have been regarded as potential agents for Photodynamic Therapy (PDT) [1,8], being an alternative, to the classical porphyrins and porphyrins-based photosensitizers [1]. Despite the many commercially available fluorescence dyes, they still suffer from shortcomings, such as low fluorescence quantum yields (QYs) and insufficient photostability. Also, there is a need for not only brightly fluorescent dyes but also truly dark quenchers for energy transfer measurements

* Corresponding author. Tel.: +48 52 374 9112; fax: +48 52 374 9005.

E-mail address: nina@utp.edu.pl (J. Kabatc).

that exhibit no residual fluorescence. In particular, in the red region, the lack of bright, photostable markers for imaging applications is still pronounced [9]. In this context, cyanine dyes are considered to be very promising candidates for PDT and the possibility to use them for this purpose critically depends on their photophysical and photochemical properties. These include strong absorption ($>10^5 \text{ M}^{-1} \text{ cm}^{-1}$) within the so-called “phototherapeutic window” (600–1100 nm), in which tissue light scattering is low and light penetration in tissues increases, and an inherent ability to generate cytotoxic oxygen from ground-state triplet oxygen [1].

Long-wavelength absorbing labels are of substantial interest because red and near-infrared (NIR) light penetrates more deeply into biological materials and generates much less background fluorescence than short-wavelength light [10,11]. Cyanine dyes are a prominent class of fluorescent dyes that – depending on their molecular structure – cover the whole spectrum from the blue to the NIR.

Some hemicyanine dyes derived from 2-methylbenzothiazole and its derivatives display poor photostability and low water-solubility. It is well known, that the water-solubility of fluorescence probes is a significant issue in biological applications.

Herein we report the synthesis of some new hemicyanine dyes **2a**, **2b** and **2c** (Scheme 1), displaying absorption about 520 nm, in which structural variation as the type of substituent in styryl moiety was made, envisioning their potential usefulness as PDT sensitizers.

Hemicyanine dyes have traditionally been synthesized by condensation between *N*-alkyl heterocyclic bases, containing an activated methyl group in the 2-position in relations to the quaternary ammonium salt and aromatic aldehyde.

Experimental section

Materials and general methods

All reagents used for the synthesis of dyes (2-methylbenzothiazole, 3-iodopropionic acid, *p*-(*N,N*-dimethylamino)benzaldehyde, *p*-(*N,N*-diethylaminobenzaldehyde) and 4-(1-pyrrolidinyl)benzaldehyde), bovine serum albumin (BSA), and solvents (spectroscopic grade) were purchased from Aldrich (Poland) and were used without further purification.

Reactions were monitored by thin-layer chromatography (TLC) using 0.25 mm aluminum-backed silica-gel plates (Merck 60 F₂₅₄). The TLC plates were eluted with CH₂Cl₂ or CH₂Cl₂/MeOH (9/1).

Melting points were measured on the Boëthius apparatus (type PHMK 05, Germany).

¹H and ¹³C NMR spectra were recorded in DMSO-*d*₆ on a Varian Gemini 200 spectrometer operating at 200 MHz. Chemical shifts are reported in ppm using TMS as an internal standard. Coupling constants (*J*) are given in Hz.

IR spectra were recorded on a Bruker Vector 22 FTIR Spectrometer (Germany). All samples were prepared by mixing FTIR-grade KBr (Sigma-Aldrich) with 1% (w/w) dye, and grinding to a fine powder. Spectra were recorded over the 400–4000 cm^{−1} range. Characteristic absorptions are given in cm^{−1}.

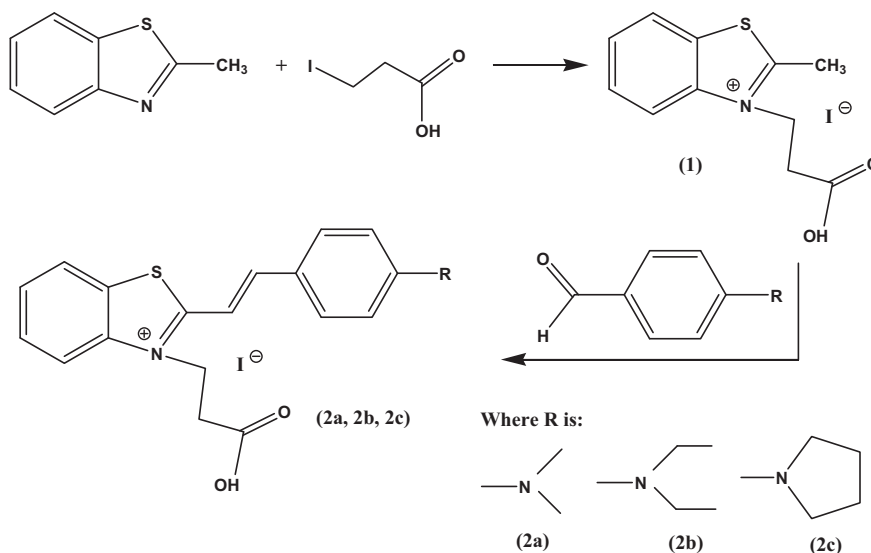
The elemental analysis was made with a Vario MACRO 11.45-0000, Elementar Analyser Systeme GmbH (Germany), operating with the software VARIOEL 5.14.4.22.

UV/Vis spectra were performed on a Varian Carry 50 Spectrophotometer using following solvents: water, dimethylsulfoxide (DMSO), acetonitrile, methanol and acetone. The measurements were performed at room temperature. Wavelength of maximum absorption is reported in nm.

Fluorescence measurements were performed on a UV-VIS-NIR Fluorolog 3 Spectrofluorimeter (Horiba Jobin Yvon).

Aggregation

The absorption spectra display no obvious change when the concentrations of the dyes solution are lower than 1 μM. Otherwise, when the concentration is higher than 40 μM, the dyes tend to deposit from the solutions. So 1–40 μM were chosen as the testing concentration ranges for all dyes. The formation of aggregates leads to a change in the wavelength maxima and shape of the absorption band which can be used to recognize the occurrence of aggregation. The absorption intensity is proportional to the concentrations of the dyes in low concentration, but the aggregation will make the absorption density of the monomer decrease, so the spectra are normalized (each spectrum data divided by its maximum absorption value) in order to facilitate direct comparisons on the shapes of the spectra. The loss of monomer absorption relative to 1 μM can indicate the relative amount of aggregated molecules.



Scheme 1. Synthesis of *N*-(carboxyethyl)-2-methylbenzothiazole-based dyes.

Photostability

The photostability tests were carried out in quartz cell (10 mm) where sample solution was irradiated with an argon laser using the visible emission (514 nm) of the air-cooled Ion Laser Systems model 177-G01 (Spectra-Physics, USA) at room temperature. The average power of irradiation was 400 mW. Measurements were performed in aqueous solution of the dye. The optical density at the long-wavelength maximum was controlled. The solutions were placed approximately 350 mm from an ion argon laser and irradiated with continuous stirring. The 5 μ M solutions of the dyes in water were irradiated and the irreversible bleaching of the dyes at the absorption peak was monitored as a function of time. The absorption spectra were measured before irradiation and during light exposure. The relative photostabilities were calculated as the ratio between the measured absorbances at the long-wavelength maximum before and after exposure (A/A_0), and the corresponding plots were generated.

Redox potential

The reduction potentials were measured by cyclic voltammetry. An Electroanalytical MTM System model EA9C-4z (Poland), equipped with a small-volume cell, was used for the measurements. A 1 mm platinum electrode was applied as the working electrode. A platinum wire constituted the counter electrode, and a silver/silver chloride (Ag/AgCl) electrode served as a reference. The supporting electrolyte was 0.1 M tetrabutylammonium perchlorate in dry acetonitrile. The solution was deoxygenated by bubbling argon gas through the solution. The potential was swept from -1.8 to 1.8 V at a rate of 500 mV/s to record the current-voltage curve.

Dye-BSA association

The association of dye and bovine serum albumin (BSA) in buffer solution (TRIS-HCl, pH = 7.0) was conducted. The concentration of the dyes was kept constant at 20.0 μ M. To the dye solution the solution of BSA with increasing concentrations was added. Then after 20 min, the absorption spectra of dyes were recorded. The BSA concentrations were equal: 0; 2×10^{-6} M; 3×10^{-6} M; 7×10^{-6} M; 13×10^{-6} M; 16×10^{-6} M; 20×10^{-6} M; 27×10^{-6} M; 30×10^{-6} M; 40×10^{-6} M; 7.5×10^{-5} M; 10.5×10^{-5} M; 13.5×10^{-5} M. The measurements were performed at room temperature.

Synthesis

The synthetic routes of the dyes are shown in Scheme 1. 2-Methylbenzothiazole quaternized salt (**1**) was synthesized according to the literature procedure [12] heating under reflux a solution of 2-methylbenzothiazole and appropriate alkyl iodide in acetonitrile as a solvent.

Synthesis of *N*-(carboxyethyl)-2-methylbenzothiazolium iodide (**1**)

To an acetonitrile solution (50 mL) of 2-methylbenzothiazole (5 mmol, 6.4 mL), 12 g of 3-iodopropionic acid (6 mmol) was added. The mixture was refluxed for 30 h. After cooling, the resulting light yellow precipitate was filtered, washed with ether and dried on the air.

Yield: 11.44 g (66.0%), m.p. 229–230 °C.

^1H NMR (DMSO- d_6), δ (ppm): 2.926–2.998 (t, 2H, CH_2); 3.237 (s, 3H, CH_3); 4.835–4.906 (t, 2H, $\text{N}-\text{CH}_2$); 7.734–7.900 (2H, Ar); 8.319–8.442 (2H, Ar); 12.714 (1H, $-\text{OH}$). ^{13}C NMR (DMSO- d_6), δ (ppm): 1.61; 27.65; 87.407; 105.439; 111.92; 115.47; 121.296; 123.08; 123.89; 127.84; 128.323; 128.849; 129.379; 132.893;

171.378. Anal. Calcd. for: $\text{C}_{11}\text{H}_{12}\text{NSO}_2\text{I}$: C, 37.82; H, 3.43; N, 4.01. Found: C, 37.71; H, 3.47; N, 4.12.

General procedure for the synthesis of dyes

A solution of the quaternary ammonium salt (**1**) (1.0 mmol) and appropriate benzaldehyde (1.0 mmol) in 5 mL of ethanol with few drops of piperidine was heated under reflux for few hours. The precipitated crystals were collected by filtration at reduced pressure. The solid dye was washed several times with 200 mL of diethyl ether and dried on the air. The physical and spectral data are shown below.

N-(Carboxyethyl)-2-[4-(*N,N*-dimethylamino)styryl]benzothiazolium iodide (**2a**). This compound was obtained from *N*-(carboxyethyl)-2-methylbenzothiazolium iodide and *p*-(*N,N*-dimethylamino)benzaldehyde in 82.0% overall yield, as violet crystals; m.p. 226–227 °C.

^1H NMR (DMSO- d_6), δ (ppm): 2.821–2.889 (m, 2H, CH_2); 3.061 (s, 6H, CH_3); 4.874–4.944 (m, 2H, $\text{N}-\text{CH}_2$); 6.753–6.797 (d, $J = 8.8$ Hz, 1H, $-\text{CH}=\text{}$); 7.597–7.630 (d, $J = 6.6$ Hz, 2H, Ar); 7.674–7.731 (t, 2H, Ar); 7.839–7.883 (d, $J = 8.8$ Hz, 1H, $-\text{CH}=\text{}$); 7.984–8.093 (t, 2H, Ar); 8.231–8.269 (d, $J = 7.6$ Hz, 2H, Ar); 12.74 (s, 1H, OH). ^{13}C NMR (DMSO- d_6), δ (ppm): 22.223 (CH_2); 32.445 (CH_2); 39.782 (CH_3); 43.905 ($\text{N}-\text{CH}_2$); 106.021 (CH); 111.811 (CH); 115.807 (CH); 123.781 (CH); 127.294 (CH); 128.805 (CH); 132.892 (CH); 150.406 (CH); 171.469 (COOH). IR (KBr) ν (cm^{-1}): 3629, 3510, 3332 (OH); 3068 (Ar); 3007 (COOH); 2919, 1487, 1462, 1446 ($-\text{CH}_2-$); 2827 ($\text{N}-\text{CH}_3$); 2367 ($\text{C}=\text{N}^+$), 1993 ($\text{ArS}-\text{C}$); 1720 ($\text{C}=\text{O}$); 1615 ($\text{C}=\text{C}$); 1580 (R_3N^+); 2919; 1462; 1446 ($-\text{CH}_3$); 1188 ($\text{C}-\text{N}$). Anal. Calcd. for: $\text{C}_{20}\text{H}_{21}\text{N}_2\text{SO}_2\text{I}$: C, 50.00; H, 4.37; N, 5.83. Found: C, 50.11; H, 4.39; N, 5.88.

N-(Carboxyethyl)-2-[4-(*N,N*-diethylamino)styryl]benzothiazolium iodide (**2b**). It was obtained from *N*-(carboxyethyl)-2-methylbenzothiazolium iodide and *p*-(*N,N*-diethylamino)benzaldehyde in 79.0% overall yield, as navy blue crystals; m.p. 198–200 °C.

^1H NMR (DMSO- d_6), δ (ppm): 1.119–1.187 (t, 6H, $-\text{CH}_3$); 2.853–2.921 (m, 2H, CH_2); 3.452–3.537 (m, 4H, CH_2); 4.890–4.959 (t, 2H, CH_2); 6.800–6.844 (d, $J = 8.8$ Hz, 1H, $-\text{CH}=\text{}$); 7.748–7.708 (d, $J = 8.0$ Hz, 2H, Ar); 7.748–7.785 (t, $J = 7.4$ Hz, 2H, Ar); 7.862–7.906 (d, $J = 8.8$ Hz, 1H, $-\text{CH}=\text{}$); 8.073–8.113 (d, $J = 8.0$ Hz, 2H, Ar); 8.248–8.287 (d, $J = 7.8$ Hz, 2H, Ar); 12.673 (s, 1H, OH). ^{13}C NMR (DMSO- d_6), δ (ppm): 12.574 (CH_2); 32.391 (CH_2); 43.823 (CH_2); 44.242 ($\text{N}-\text{CH}_2$); 105.457 (CH); 111.547 (CH); 115.725 (CH); 123.762 (CH); 127.167 (CH); 128.778 (CH); 133.384 (CH); 150.369 (CH); 171.451 (COOH). IR (KBr) ν (cm^{-1}): 3588, 3519 (OH); 2974 (Ar); 2902 (COOH); 1488, 1462, 1448 ($-\text{CH}_2-$); 2621, 2572 ($\text{N}-\text{CH}_2$); 2366 ($\text{C}=\text{N}^+$), 1994 ($\text{ArS}-\text{C}$); 1733 ($\text{C}=\text{O}$); 1685, 1654 1648 ($\text{C}=\text{C}$); 1576 (R_3N^+); 1462; 1446 ($-\text{CH}_3$); 1186 ($\text{C}-\text{N}$). Anal. Calcd. for: $\text{C}_{22}\text{H}_{25}\text{N}_2\text{SO}_2\text{I}$: C, 51.97; H, 4.92; N, 5.51. Found: C, 52.00; H, 4.93; N, 5.48.

N-(2-Carboxyethyl)-2-[4-(pyrrolidinyl)styryl]benzothiazolium iodide (**2c**). Obtained from *N*-(carboxyethyl)-2-methylbenzothiazolium iodide and 4-(1-pyrrolidinyl)benzaldehyde in 45.0% overall yield, as dark violet crystals; m.p. 244–245 °C.

^1H NMR (DMSO- d_6), δ (ppm): 1.985 (t, 4H, CH_2); 2.886 (t, 2H, CH_2); 3.156–3.401 (t, 4H, $\text{N}-\text{CH}_2$); 4.915 (t, 2H, $\text{N}-\text{CH}_2$); 6.650–6.692 (d, $J = 8.4$ Hz, 1H, $-\text{CH}=\text{}$); 7.665–7.703 (d, $J = 7.6$ Hz, 2H, Ar); 7.743–7.780 (t, $J = 7.4$ Hz, 2H, Ar); 7.871–7.913 (d, $J = 8.4$ Hz, 1H, $-\text{CH}=\text{}$); 8.064–8.102 (d, $J = 7.6$ Hz, 2H, Ar); 8.243–8.281 (d, $J = 7.6$ Hz, 2H, Ar); 12.740 (s, 1H, OH). ^{13}C NMR (DMSO- d_6), δ (ppm): 24.881 (CH_2); 32.382 (CH_2); 43.796 (CH_2); 47.656 ($\text{N}-\text{CH}_2$); 105.339 (CH); 112.275 (CH); 115.688 (CH); 123.726 (CH); 127.139 (CH); 128.751 (CH); 133.174 (CH); 150.651 (CH); 171.451 (COOH). IR (KBr) ν (cm^{-1}): 3528, 3353, 3188 (OH); 3005 (Ar); 2971 (COOH);

2921, 1488, 1454 ($-\text{CH}_2-$); 2669, 2573 ($\text{N}-\text{CH}_2$); 2347 ($\text{C}=\text{N}^+$), 1988 ($\text{ArS}-\text{C}$); 1735 ($\text{C}=\text{O}$); 1615 ($\text{C}=\text{C}$); 1575 (R_3N^+); 1455 ($-\text{CH}_3$); 1189 ($\text{C}-\text{N}$). Anal. Calcd. for: $\text{C}_{22}\text{H}_{23}\text{N}_2\text{SO}_2\text{I}$: C, 52.17; H, 4.55; N, 5.53. Found: C, 52.20; H, 4.63; N, 5.58.

Results and discussion

Synthesis of dyes

Our efforts to synthesize hemicyanine dyes bearing benzothiazole nucleus by the usual basic catalyzed condensation between a suitable quaternary ammonium salt (**1**) and three different benzaldehydes (Scheme 1). By the aforementioned procedure three new hemicyanine dyes have been prepared. The reactions provided moderate yields ranging from 45.0% to 82%.

Spectral properties

The spectral data of new dyes in different solvents are shown in Table 1.

Typical absorption and emission spectra of the dyes in different solvents are illustrated in Fig. 1.

In order to facilitate of comparison of all spectra recorded, the spectra are normalized relative to corresponding spectra in water. New hemicyanine dyes absorb (between 400 nm and 600 nm) and emit (between 550 nm and 680 nm) over a wide spectral range and extinction coefficients ranging from $4.15 \times 10^4 \text{ M}^{-1} \times \text{cm}^{-1}$ to $7.9 \times 10^4 \text{ M}^{-1} \times \text{cm}^{-1}$ (Table 1). The extinction coefficients are of the same order as for some of the most common fluorophores in this spectral region, which makes these dyes compatible not only with the green 532 nm, yellow 589 nm – diode lasers but also with blue diode lasers and light-emitting diodes at 436 nm. As shown in Fig. 1, the absorption spectra of dyes studied are characterized by one broad absorption band with maximum about 520 nm. The spectra recorded in water have several nanometers blue-shift comparing to those obtained in organic solvents. The shapes of the spectra are similar with those obtained in organic solvents.

The emission spectra showed a quite good mirror relationship with the absorption spectra and the Stokes shifts were rather small from 1850 to 2350 cm^{-1} . These characteristics are usual for polymethine dyes and suggest that only minor structural changes take place in the S_1 state of the solvated dye, relative to the S_0 state, during the fluorescence lifetime. From the time resolved fluorescence spectroscopy it is seen that the electronic excitation of dyes under study leads to short-lived excited singlet state formation. The fluorescence lifetime depends on the dye structure and ranges

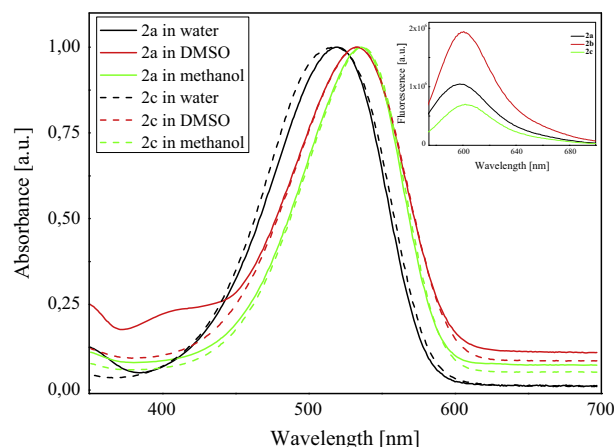


Fig. 1. Comparison of the normalized absorption spectra of dyes **2a** and **2c** in water, dimethylsulfoxide (DMSO) and methanol. Inset: The fluorescence spectra of dyes **2a**, **2b**, **2c** in acetonitrile.

from 47–84 ns. The example of kinetic curve of fluorescence decay is shown in Fig. 2.

Aggregation process

The aggregation of polymethine dyes is extremely favored by strong attractive dispersion forces derived from the high

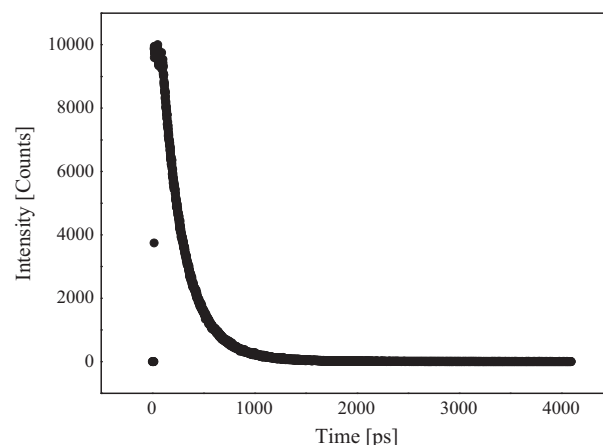


Fig. 2. The fluorescence decay recorded for dye **2a** observed in acetonitrile as a solvent.

Table 1

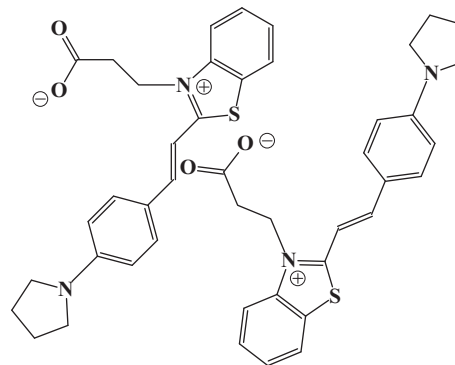
The spectral data of new dyes in different solvents.

Dye	Solvent	Absorption/emission (nm)	Stokes shift (cm^{-1})	$\epsilon (\times 10^4 \text{ M}^{-1} \text{ cm}^{-1} \text{ dm}^3)$	$\tau_f (\times 10^{-9} \text{ s})$
2a	Acetone	527	2345	5.6	84.3
	Methanol	525		5.53	
	Acetonitrile	526/600		4.43	
	Dimethylsulfoxide	523		5.34	
	Water	507		4.74	
2b	Acetone	534	1886	6.7	46.7
	Methanol	536		6.15	
	Acetonitrile	539/600		7.36	
	Dimethylsulfoxide	533		5.07	
	Water	520		4.15	
2c	Acetone	540	1852	7.47	50.9
	Methanol	537		7.9	
	Acetonitrile	540/600		6.96	
	Dimethylsulfoxide	533		6.23	
	Water	518		5.34	

polarizability of the chromophoric chain in aqueous solution [13]. Moreover, the high dielectric constant of water facilitates the aggregation process [14–16]. In this paper, the aggregates were detected through recording the absorption spectra of increasing concentration of the dyes in water in order to facilitate the formation of aggregates. UV–vis absorption spectra were recorded for solution of the dye (from 1.0 to 40 μM). Normalized absorption spectra of dye **2a**, **2b** and **2c** are shown in Fig. 3.

The spectra presented in Fig. 3 show the broad absorbance band centered around 520 nm, that strongly suggest that the dye forms water-soluble aggregates [13]. Previous reports attribute broad absorbances such as those seen for aqueous dye solution to aggregates and sharper bands to monomers arising from the dissociation of the dye aggregates in organic solvents [13,14]. While two types of aggregates, *J* (head-to-tail) and *H* (parallel), have been reported, *H*-type aggregates are frequently observed at low solution concentrations and in crystal structures [17]. The normalized absorption spectra of dyes **2a** and **2b** overlap completely which implies that non aggregates have formed. On the other hand, in a case of dye **2c**, when the concentration of dye in water achieved values higher than 5 μM the hypsochromic shift of the absorption band is observed. This behavior is attributed to the formation of *H*-aggregates formation. The absorption band becomes broad at the expense of a rise of relative intensity of it is increased [14,18].

The most probable structure of dye **2c** aggregates, according to work [19] is presented below (given is the disposition of two molecules in the aggregate):



Such a structure must be advantageous, in as much as monomeric molecules in the associate are held at both ends by weak electrostatic forces of attraction between opposite-sign charges: the positively charged nitrogen atom in heterocyclic ring of one molecule is oriented above the negative charged oxygen atom of the other molecule and vice versa. From results obtained it is seen, that an introduction of carboxylic group into dye molecule elevates its solubility in water, which hinders formation of aggregates.

Basing on this, one can conclude that the introduction of *N*-(carboxyethyl) group inhibits the aggregation of hemicyanine dyes in water, which is beneficial to their application in aqueous media.

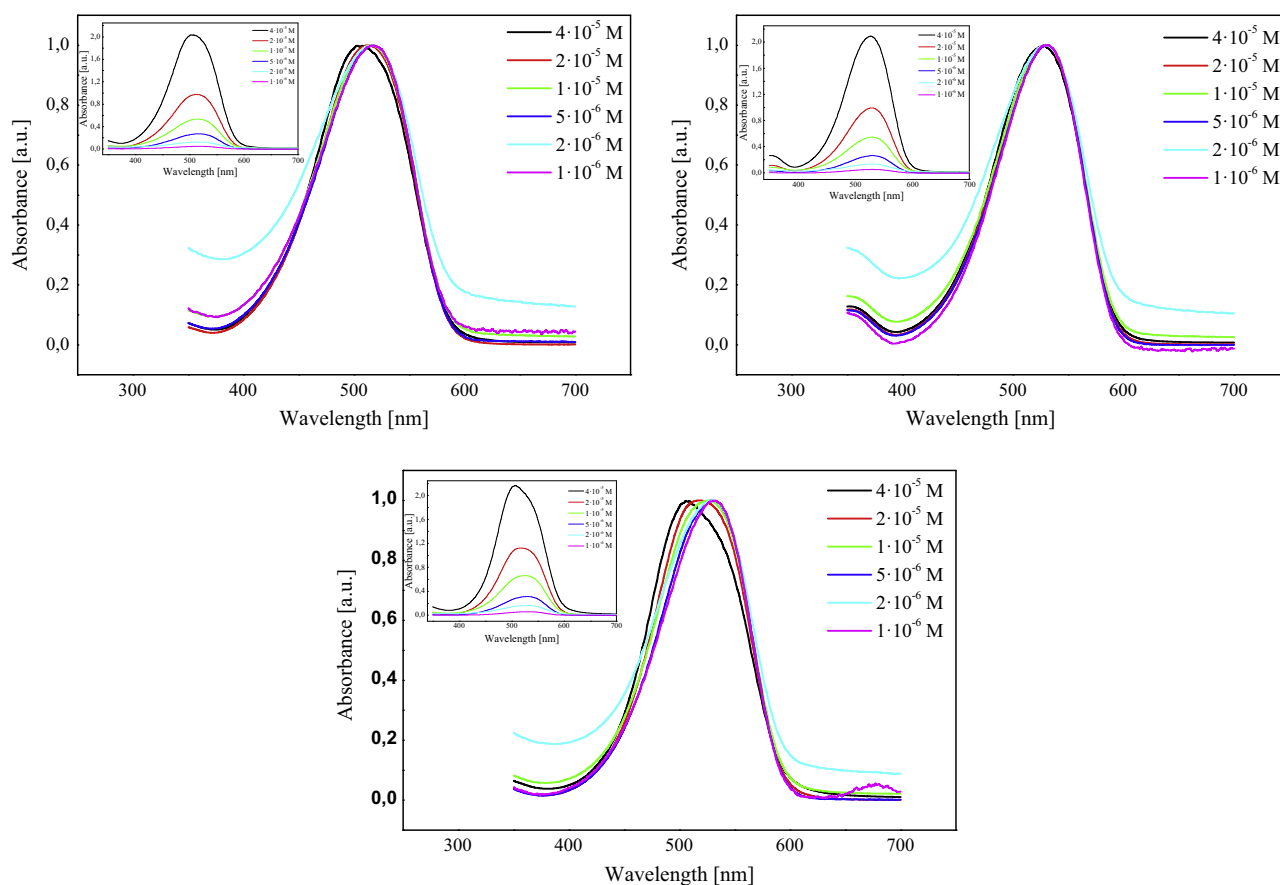


Fig. 3. Normalized absorption spectra of dyes **2a**, **2b** and **2c** in different concentrations in water: 1 (pink line), 2 (cyan line), 5 (blue line), 10 (green line), 20 (red line) and 40 μM (black line). Inset: The electronic absorption spectra before being normalized. (For interpretation of the references to color in this figure legend, the reader is referred to the web version of this article.)

Photostability

The results of photostability of the dyes are shown in Fig. 4.

After irradiation with argon laser for 7 h, the absorption intensities of **2a**, **2b** and **2c** decreases to 83.4%, 74% and 69.6% from 100%. The photostability of the novel hemicyanine dyes with *N*-(carboxyethyl) group depends on the type of substituent in the *p*-position of phenyl ring. The best photostability possess dye with *N,N*-dimethylamino group in styryl moiety.

The decomposition pathway of polymethine dyes had been depicted in the literature. Singlet oxygen was an important oxidation species which could be produced in situ by irradiation of dyes [14,20] and bleach polymethine dyes through destroying the conjugation of the dyes. On the other hand, it was reported that the quenching of singlet oxygen by polymethine dyes depends on the redox properties of dye. This process decreases as the oxidation potential of the polymethine dye increases [14,21]. The cyclovoltammograms recorded for dyes under study are presented in Fig. 5.

As it is seen in Fig. 5, the oxidation potentials of dyes studied ranging from 0.428 eV to 0.860 eV. The oxidation potential of dye possessing the pyrrolidinyl substituent in styryl moiety (**2c**) is more positive than that of dyes: **2a** and **2b**. This suggests that this dye should be less susceptible to reaction with singlet oxygen, i.e. the oxidation of this dye by singlet oxygen will not be easy to carry out. The kinetic results obtained during the photobleaching process do not confirm this observation. Therefore, one can conclude that other deactivation processes (for example: fluorescence, photoisomerization) of the excited singlet state of new dyes compete with the reaction of singlet oxygen with excited dye.

Dye-bovine serum albumin (BSA) association

It was suggested that hemicyanine dyes occupy a common hydrophobic binding site on protein to form dye-protein complex [14,20], which may change the spectroscopic properties of the dyes and be used for the determination of proteins. The electronic absorption spectra of selected dyes **2a** and **2b** associated with different concentration of bovine serum albumin (BSA) are shown in Figs. 6 and 7.

The absorbance of dyes decreased by adding bovine serum albumin in pH = 7 as expected. It is seen that upon introduction of increasing concentrations of bovine serum albumin into buffer solution of dyes **2a** and **2b** there takes place a drop of the intensity of the initial absorption band of hemicyanine dyes with $\lambda_{\max} = 507$ nm and 520 nm for dyes **2a** and **2b**, respectively, and appearance of growth short-wavelength band with λ_{\max} about

360 nm (Figs. 6 and 7). At that in electronic absorption spectra an isosbestic point is observable, which points to a simple equilibrium described by Eq. (1), between free and bound dye.

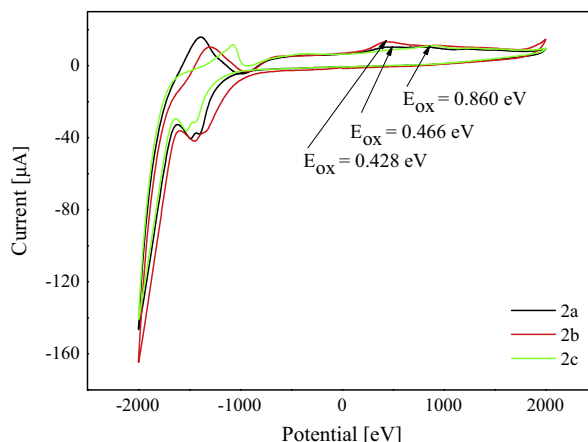


Fig. 5. Cyclic voltammograms of new hemicyanine dyes in 0.1 M tetrabutylammonium perchlorate solution in dry acetonitrile as the supporting electrolyte.

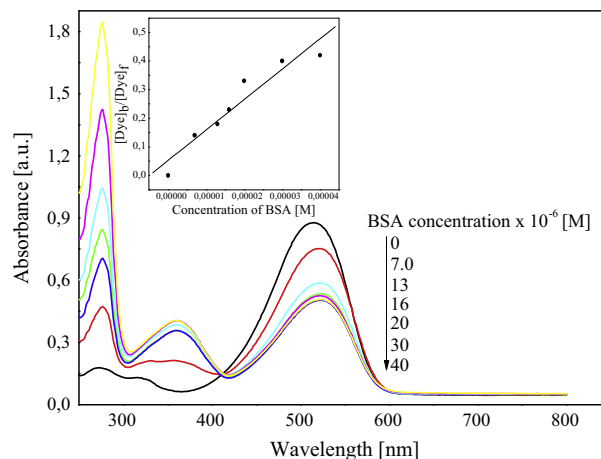


Fig. 6. Absorption spectra of dye **2a** (20 μM) in buffer solution in presence of increasing concentrations of bovine serum albumin, [BSA] = 0; 7.0; 13.0; 16.0; 20.0; 30.0; 40.0 μM. Inside: The plot of the ratio $[Dye]_b/[Dye]_f$ as a function of BSA concentrations 0–40.0 μM in pH = 7.0 (TRIS-HCl).

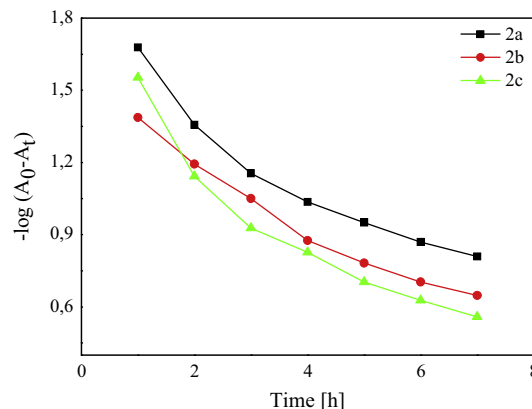
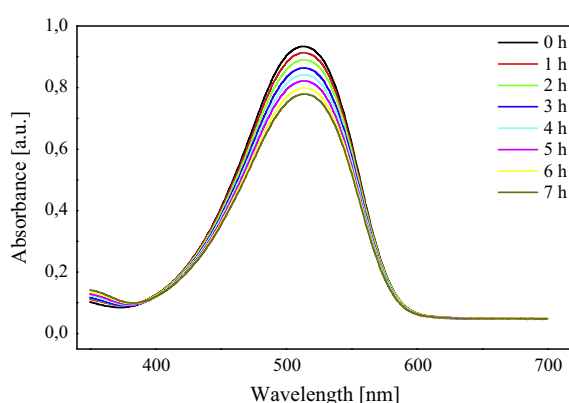


Fig. 4. Left: The changes in the electronic absorption spectra of *N*-(carboxyethyl)-2-[4-(*N,N*-dimethylamino)styryl]benzothiazolium iodide (**2a**) in water as a solvent during irradiation with argon ion laser. Right: The comparison of the photostability of all dyes studied in water.

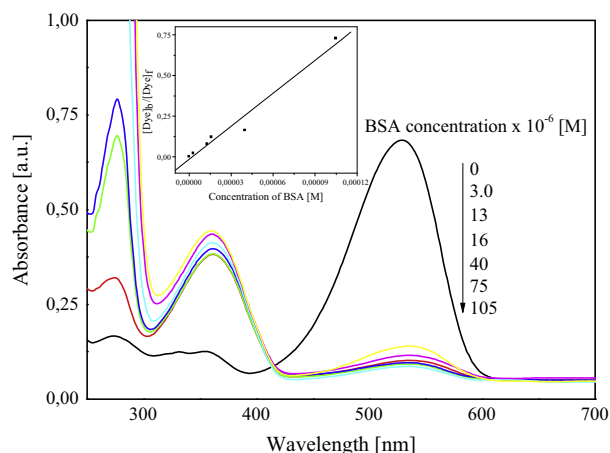


Fig. 7. Absorption spectra of dye **2b** (20 μM) in buffer solution in presence of increasing concentrations of bovine serum albumin, [BSA] = 0; 7.; 3.0; 13.0; 16.0; 40.0; 75.0 and 105.0 μM . Inside: The plot of the ratio $[\text{Dye}]_b/[\text{Dye}]_f$ as a function of BSA concentrations 0–105.0 μM in pH = 7.0 (TRIS–HCl).

The ratio of concentration of dye complexed with bovine serum albumin ($[\text{Dye}]_b$) and concentration of dye unbounded ($[\text{Dye}]_f$) as a function of BSA concentration is shown inside Figs. 6 and 7. The best linear relationship ($r^2 = 0.96$) between the ratio $[\text{Dye}]_b/[\text{Dye}]_f$ and the BSA concentration was observed in the range from 0 to 40.0 μM for dye **2a**. In the case of dye **2b**, better linear relationship ($r^2 = 0.99$) between the ratio $[\text{Dye}]_b/[\text{Dye}]_f$ and the BSA concentration was observed for wide range of bovine serum albumin concentration, e.g. from 0 to 105.0 μM . The aggregation of dye **2c** leads to the nonlinear and sigmoidal calibration curves. These two features are disadvantages for the reagents used for the absorbance and fluorescence spectrometry and for the other analytical methods during the biomolecules measurement [14,22,23]. The sensitivity of dye **2b** is higher than dye **2a**. However, the linear range is larger (0–105.0 μM). Contrary, dye **2a** is very sensitive in low concentrations of BSA, while the linear range is smaller (0–40.0 μM).

The constant of binding of monomeric dyes with bovine serum albumin K_{eq} and the binding number n were determined from the equilibrium:



where Dye and BSA are molecules of dye and bovine serum albumin respectively, n is the number of dyes molecules binding with one albumin molecule (assumed is identity of binding centers), and

$$K_{eq} = \frac{[\text{Dye} \cdot \text{BSA}]}{[\text{Dye}]_f [\text{BSA}]_f} = \frac{[\text{Dye}]_b}{[\text{Dye}]_f [\text{BSA}]_f} \quad (2)$$

where $[\text{Dye}]_b = [\text{DyeBSA}]$ and $[\text{Dye}]_f$ are concentrations of bound and free dye respectively; $[\text{BSA}]_f$ is concentration of free bovine serum albumin. $[\text{Dye}]_b$ and $[\text{Dye}]_f$ at that were determined by means of modeling the absorption spectra of the dye + albumin system as the sum of spectra of free (at $[\text{BSA}] = 0$) and bound (at large $[\text{BSA}]$) forms of the dye [19].

The constant of binding of monomeric dyes with bovine serum albumin, K_{eq} obtained from experimental relationship $[\text{Dye}]_b/[\text{Dye}]_f$ and $[\text{BSA}]$ and on the assumption of $n=1$ equals $1.06 \times 10^4 \text{ M}^{-1}$ and $1.89 \times 10^4 \text{ M}^{-1}$ for dyes **2a** and **2b**, respectively. The K_{eq} values calculated for dyes tested from the change in dye absorption spectra assuming $n = 1$ are much lower than squaraine dyes [19]. The low apparent value of n at that, testifies to significant aggregation of hemicyanines tested on bovine serum albumin and weak interaction of dye with bovine serum albumin. Therefore, one can conclude, that the processes of binding

of monomeric dye with albumin and aggregation of dye molecules on albumin may be regarded as competing ones: when monomeric binding is weak, aggregation manifests itself strongly, and vice versa [19]. Tatikolov and co-workers [19,24] have established earlier, studying the interaction of polymethine dyes with human serum albumin, that for good complex formation of a polymethine dye with albumin first of all necessary is a negative charge of the dye (albumin binding centers have probably a positive charge). Besides, a role is played as well by hydrogen bonds, which the dye can form with biomolecule binding centers. This was observed by Tatikolov for anionic oxonols [24].

Conclusion

In summary, we have synthesized three new hemicyanine dyes containing *N*-carboxyethyl-2-benzothiazolium moiety and tested their properties such as absorption, fluorescence, photostability and spectroscopic response to BSA. The results showed that the introduction of the pyrrolidinyl group in *p*-position of phenyl ring in styryl moiety increase the aggregation of the dye in water solution and results in decrease the trend of the association with bovine serum albumin. Among the dyes, **2a** and **2b** with *N,N*-dimethylamino and *N,N*-diethylamino group in styryl moiety have high photostability and excellent linear relationship between absorption properties of dye and bovine serum albumin concentration.

It has been shown that dyes studied can bind to bovine serum albumin and possess sufficient high photostability. This makes the given dyes quite promising for application in the capacity of label probes for biomolecules which connection the study of non-covalent interactions of new hemicyanine dyes with biomolecules appears quite topical.

These positive results arising from the introduction of both *N*-carboxyethyl and *N,N*-dimethylamino or *N,N*-diethylamino groups would be worthwhile to design new hemicyanine dyes with powerful functions for their wide applications.

Acknowledgement

This work was supported by The National Science Centre (NCN) Grant No. 2013/11/B/ST5/01281.

References

- [1] S.S. Ramos, P.F. Santos, L.V. Reis, P. Almeida, *Dyes Pigm.* 53 (2002) 143–152.
- [2] W. West, *Photograph. Sci. Eng.* 18 (1974) 35–48.
- [3] H. Zollinger, *Color Chemistry – Synthesis, Properties and Applications of Organic Dyes and Pigments*, second ed., VCH Publishers, Weinheim, 1991.
- [4] D.M. Sturmer, D.W. Heseltine, in: T.H. James (Ed.), *Sensitizing and Desensitizing Dyes – The Theory of Photographic Processes*, fourth ed., Macmillan, New York, 1977.
- [5] M. Matsuoka (Ed.), *Infrared Absorbing Dyes*, Plenum Press, New York, 1990.
- [6] M. Okawara, T. Kitao, T. Hirashima, M. Matsuoka, *Organic Colorants – A Handbook of Data of Selected Dyes for Electro-Optical Applications*, Elsevier Science Publishers B.V., Amsterdam, 1988.
- [7] J. Fabian, H. Nakazumi, W. Matsuoka, *Chem. Rev.* 92 (1992) 1197–1226.
- [8] Z. Diwu, W. Lown, *Pharmac. Ther.* 63 (1994) 1–35.
- [9] L. Patsenker, A. Tatarets, O. Kolasova, O. Obukhova, Y. Povrozin, I. Fedyunyayeva, I. Yermolenko, *Ann. NY. Acad. Sci.* 11 (2008) 179–187.
- [10] J.N. Miller, *Long-Wavelength and Near-Infrared Fluorescence: State of the Art, Future Applications, and Standards*, Springer, Berlin, 2008.
- [11] H.H. Gorris, S.M. Saleh, D.B.M. Groegel, S. Ernst, K. Reiner, H. Mustroph, O.S. Wolfbeis, *Bioconjug. Chem.* 22 (2011) 1433–1437.
- [12] T. Dentani, *Dyes Pigm.* 77 (2008) 59–69.
- [13] S. Saito, T.L. Massie, T. Maeda, H. Nakazumi, Ch.L. Colyer, *Anal. Chem.* 84 (2012) 2452–2458.
- [14] B. Wang, J. Fan, S. Sun, L. Wang, B. Song, X. Peng, *Dyes Pigm.* 85 (2010) 43–50.
- [15] A.K. Cibisov, G.V. Zakharova, H. Gerner, *Phys. Chem. Chem. Phys.* 3 (2001) 44–49.
- [16] R.S. Grynyov, A.V. Sorokin, G.Y. Guralchuk, S.L. Yefimova, I.A. Borovoy, Y.A. Malyukin, *J. Phys. Chem. C* 112 (2008) 20458–20462.
- [17] A.W. Lantz, Y. Bao, D.W. Armstrong, *Anal. Chem.* 79 (2007) 1720–1724.

- [18] A.S. Tatikolov, S.M.B. Costa, J. Photochem. Photobiol., A 140 (2001) 147–156.
- [19] A.S. Tatikolov, I.G. Panova, A.A. Ishchenko, M.A. Kudinova, Biophysics 55 (2010) 35–40.
- [20] C. Kanony, B. Akerman, E. Tuite, J. Am. Chem. Soc. 123 (2001) 7985–7995.
- [21] J.R. Kanofsky, P.D. Sima, Photochem. Photobiol. 71 (2000) 361–368.
- [22] F. Meadows, N. Narayanan, G. Patonay, Talanta 50 (2000) 1149–1155.
- [23] Y. Suzuki, K. Yokoyama, J. Am. Chem. Soc. 127 (2005) 17799–17802.
- [24] A.S. Tatikolov, S.M.B. Costa, Biophys. Chem. 107 (2004) 33.